Cytochrome P450 2B6 Amperometric Biosensor for Continuous Monitoring of Propofol

David C. Ferrier*, Janice Kiely, Richard Luxton

Institute of Bio-Sensing Technology, University of the West of England, Frenchay Campus, Bristol BS16 1QY, United Kingdom

* Corresponding author: David.Ferrier@uwe.ac.uk

Abstract

Despite the growing evidence of improved patient outcomes and of a substantially reduced environmental impact of propofol-based total intravenous anesthesia when compared to volatile-based techniques, the vast majority of general anesthetics still use volatile agents for the maintenance phase. A significant reason for this is the lack of suitable point-of-care, real-time blood propofol measurement techniques. Here we present an enzyme-based electrochemical biosensor for the detection of propofol. Deactivated yeast cells expressing the enzyme cytochrome P450 2B6 are immobilized, alongside gold nanoparticles, within a chitosan film upon the surface of a screen printed electrode. In the presence of the cofactor NADPH, the enzyme converts propofol to a quinone/quinol redox pair that can be detected using simple electrochemistry. This approach avoids the issue of electrode fouling that commonly renders electrochemical propofol sensors impractical. The sensor has a limit of detection of 67 ± 7 ng/ml and a sensitivity of 4.2 ± 0.2 nA/µg/ml/mm^2. It has been successfully demonstrated in a serum-like solution and has shown a linear response across the therapeutic range of propofol (1 – 10 µg/ml). Additionally, the sensor has shown good specificity with regards to potential interfering compounds.

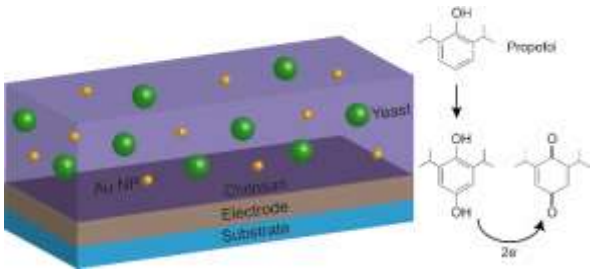

Keywords: Propofol biosensor; 2,6-diisopropylphenol sensor; cytochrome P450 2B6; electrochemical biosensor; real-time detection

1. Introduction

Propofol (2,6-diisopropylphenol) is an intravenous drug used to induce and maintain general anesthesia. Its favorable pharmacokinetic characteristics mean that it has been the most widely used intravenous anesthetic for the last thirty years [1] [2].

The most common practice in general anesthesia is to induce using intravenous methods and to maintain using volatile-based methods [3]. However, total intravenous anesthesia (TIVA), wherein anesthesia is both induced and maintained intravenously, has many benefits. For instance, there is emerging evidence that the long-term survival rates for cancer patients may be significantly improved for patients who undergo TIVA as opposed to volatile-based anesthesia [4]. Also, the most commonly used volatile anesthetics are potent greenhouse gasses with global warming potentials 2-3 orders of magnitude higher than that of carbon dioxide, meaning that TIVA (which does not require the use of these gasses) has a significantly reduced environmental impact [5] [6]. In addition, TIVA has reduced side effects when compared to volatile-based anesthesia [7]. A major obstacle to the widespread adoption of TIVA is the lack of suitable methods for direct, real-time monitoring of the propofol concentration in a patient's bloodstream. Current practice is to use models to calculate the required infusion rate based on general pharmacokinetic data and patient metrics such as weight. However, these models are not very accurate and possess significant shortcomings [3] [8]. The most common current laboratory-based methods for propofol detection include gas chromatography-mass spectroscopy (GC-MS) and high-performance liquid chromatography (HPLC), both of which possess significant limitations in terms of cost, complexity and reporting time [1] [9]. As such, there is a significant need for real-time, point-of-care propofol sensors.

Several groups have developed novel optical techniques for propofol detection, such as the spectrophotometric approach of Liu *et al.* [10] and the fluorimetric approach of Diao *et al.* [11]. However, such techniques have typically only been demonstrated for discrete, rather than continuous, measurement.

It is possible to detect propofol electrochemically, via its oxidation. However, this reaction produces radicals which undergo further reactions to produce polymeric molecules at the electrode surface [12] [13]. These polymers are insoluble and non-conductive and thus lead to significant electrode fouling. Therefore, the direct electrochemical detection of propofol is not practical for real-world applications, where any propofol sensor would be required to produce stable currents over periods of up to several hours. The group of Lindner *et al.* have attempted to overcome this challenge through the application of a plasticized polyvinyl chloride membrane [1] and Aiassa *et al.* have attempted to compensate for electrode fouling through machine learning [14].

In this paper we present an electrochemical propofol biosensor based upon the enzyme cytochrome P450 2B6. The enzyme is expressed within deactivated yeast cells, which are in turn immobilized alongside gold nanoparticles within a chitosan film upon the surface of a screen-printed electrode. Cytochrome P450 2B6 is one of the principal enzymes responsible for metabolizing propofol within the human body [15]. In the presence of the cofactors nicotinamide adenine dinucleotide phosphate (NADPH) and D-glucose-6-phosphate, the enzyme will convert propofol into a quinone/quinol redox pair [16] (Fig. 1). The NADPH acts as an electron source, allowing the enzyme to catalyze the conversion of propofol. Unlike direct electrochemical oxidation, the conversion of propofol in this manner will not lead to polymerization and therefore will not cause electrode fouling. The redox pair can be detected electrochemically, thus enabling the simple and rapid measurement of the propofol

concentration. Immobilizing the enzyme within the yeast cells preserves the stability of the enzyme, which can otherwise prove challenging. Chitosan was chosen as the means of immobilization as it is abundant, biocompatible and highly porous. The addition of the gold nanoparticles is to provide additional stabilization of the enzyme.

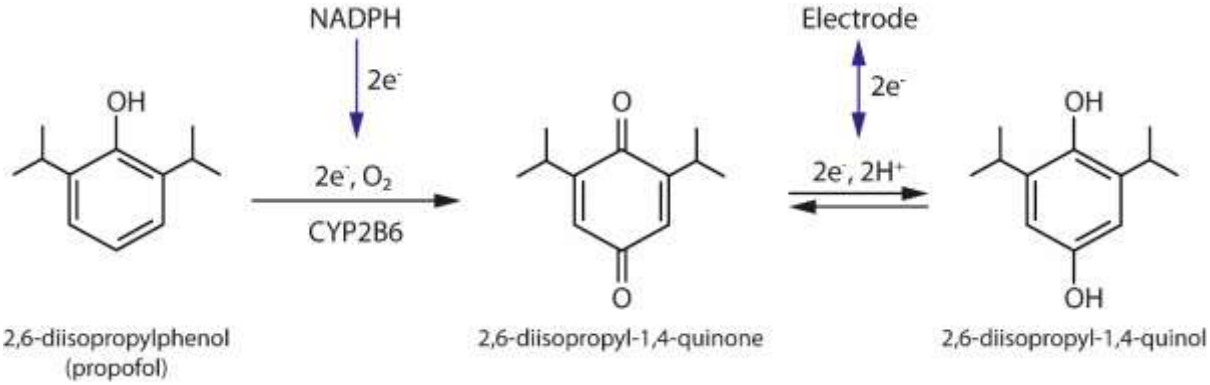

Fig. 1 – Reaction mechanism for conversion of propofol to quinone/quinol redox pair by cytochrome P450 2B6. NADPH acts as the electron source for the enzyme reaction and the electrode is used to detect the reaction products. Adapted from Shioya et al. [13].

2. Materials and methods

a. Materials

All materials were obtained from Sigma-Aldrich (Dorset, UK) and used as supplied. β-Nicotinamide adenine dinucleotide phosphate sodium salt hydrate ($NADP^+$) and D-glucose-6-phosphate dipotassium salt hydrate (G6P) were dissolved in phosphate buffered saline (PBS) (10 mM phosphate buffer, 2.7 mM KCl, 137 mM NaCl, pH 7.4) to produce solutions in which the concentration of each was 50 µg/ml. Unless stated otherwise, this was the testing solution for the electrochemical measurements described in section 2d. Solutions of identical buffer, NaCl, KCl, $NADP^+$ and G6P concentrations were also prepared with the addition of 5 wt% of bovine serum albumin (BSA) (heat shock fraction, pH 7, ≥98%). 2,6-diisopropylphenol (97%) was diluted in dimethyl sulfoxide (99.9%) to create a 10 mM stock solution. This stock was further diluted with the $NADP^+$/G6P solution to produce propofol solutions of varying concentrations as required for the tests described herein. Ascorbic acid (>99%) and lidocaine were each dissolved in dimethyl sulfoxide to produce 10 mM stock solutions and diluted in the same manner as the propofol solutions to produce 1 mM solutions.

b. Apparatus

The screen-printed electrodes used in these experiments were purchased from BVT Technologies (Strážek, Czech Republic). They constitute a three-electrode cell consisting of a 1 mm diameter graphite working electrode, a graphite counter electrode and a silver/silver chloride (Ag/AgCl) pseudo-reference electrode. All measurements were performed using a PamSens EmStat^3 potentiostat.

c. Electrode preparation

Gold nanoparticles were produced using a standard sodium citrate reduction technique [17]. Briefly, 10 mg of gold chloride hydrate ($HAuCl_4$) (99.995%) were dissolved in 20 ml of deionized water and this solution brought to boiling point under magnetic stirring. Trisodium citrate dihydrate (≥99%) was dissolved in deionized water to produce a 2.5 wt% solution and 1 ml of this solution was added to the $HAuCl_4$ solution and the mixture kept at boiling point for 5-10 minutes until it had undergone a color change to deep red, before being allowed to cool to room temperature.

CypExpress 2B6 (a deactivated, permeabilized yeast expressing cytochrome P450 2B6 and NADPH oxidoreductase) was suspended in phosphate buffer (pH 7) at a concentration of 25 mg/ml. This suspension was mixed with the gold nanoparticle solution and a 1 wt% chitosan solution (1% acetic acid) in a ratio of 1:1:2 by volume (resulting in a gold:CypExpress:chitosan ratio by mass of approximately 1:100:42). 1 µl of this mixture was drop-cast onto the working electrode of each screen-printed electrode and left to dry at 4°C. Once dry, the electrodes were immersed in 10 mM PBS for 30 minutes at room temperature, before being re-dried and stored at 4°C until use. Additional electrodes were prepared in a similar manner without the addition of gold nanoparticles. An equivalent volume of phosphate buffer (pH 7) was added in place of the gold nanoparticle solution.

d. Electrochemical measurement

Cyclic voltammetry measurements were performed by depositing 50 µl of propofol solutions of varying concentration upon the functionalized electrodes and cycling the potential between -0.8 and +1.0 V, commencing at +0.1 V, with a scan rate of 100 mV/s.

Amperometry measurements were performed by immersing the functionalized electrodes in 20 ml of 50 µg/ml $NADP^+$ and G6P solution (10 mM PBS) and measuring the current at +0.6 V. The solution was stirred magnetically and aliquots of 1 mM propofol solution were injected at regular intervals. Similar experiments were carried out injecting aliquots of 1 mM ascorbic acid and lidocaine solutions, and using $NADP^+$/G6P solutions containing 5 wt% BSA.

Control measurements were carried out by performing amperometry as above in 10 mM PBS solutions without $NADP^+$ or G6P, and injecting aliquots of 1 mM propofol solution at regular intervals. These experiments were carried out in triplicate using the same electrode. Between each run the electrode was rinsed with 10 mM PBS, dried and stored at 4°C overnight.

3. Results and discussion

Cyclic voltammetry with varying propofol concentration (Fig. 2) shows concentration dependent peaks at approximately +0.5 V and -0.2 V. This behavior is as would be expected for a quinone/quinol redox pair [18], with the peaks corresponding to the reduction of 2,6-diisopropylquinone and the oxidation of 2,6-diisopropylquinol respectively. This indicates that the enzyme within the yeast cells is converting propofol to the expected metabolites. Additionally, these results inform the selection of the potential for the amperometry measurements.

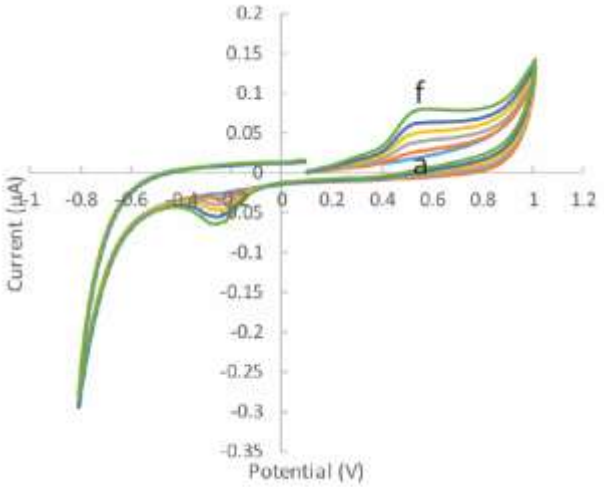

Fig. 2 – Cyclic voltammograms of solutions of propofol concentration: a) 0.00, b) 0.89, c) 1.78, d) 2.67, e) 3.57 and f) 4.47 μg/ml at a scan rate of 100 mV/s. All solutions contain 50 μg/ml NADP+ and G6P, 10 mM PBS. Potentials are vs. screen-printed Ag/AgCl.

The amperometry measurements show a clear increase in current with each injection of propofol solution (Fig. 3a). The responses are fast, reaching a plateau within two minutes, and stable throughout the experiment. The stability of the sensor response over the duration of the experiment demonstrates the absence of any electrode fouling resulting from the direct oxidation of propofol. Plotting the average plateau current against the propofol concentration (Fig. 3b) shows that the sensor produces a clear linear response to varying propofol concentration across the testing range. The sensitivity is 4.1 ± 0.2 nA/μg/ml/mm^2 with a coefficient of variation of 0.07, and the limit of detection is 67 ± 7 ng/ml, well below the lower end of the therapeutic range (typically 1 – 10 μg/ml [19]). The sensitivity was determined by dividing the gradient of the linear fit by the area of the working electrode and the limit of detection (LoD) was calculated using the equation: $LoD = 3.3 \times \sigma_{low}/gradient$, where σ_{low} is the standard deviation at a low propofol concentration. These experiments were carried out in triplicate and baseline correction has been applied to all amperometry results.

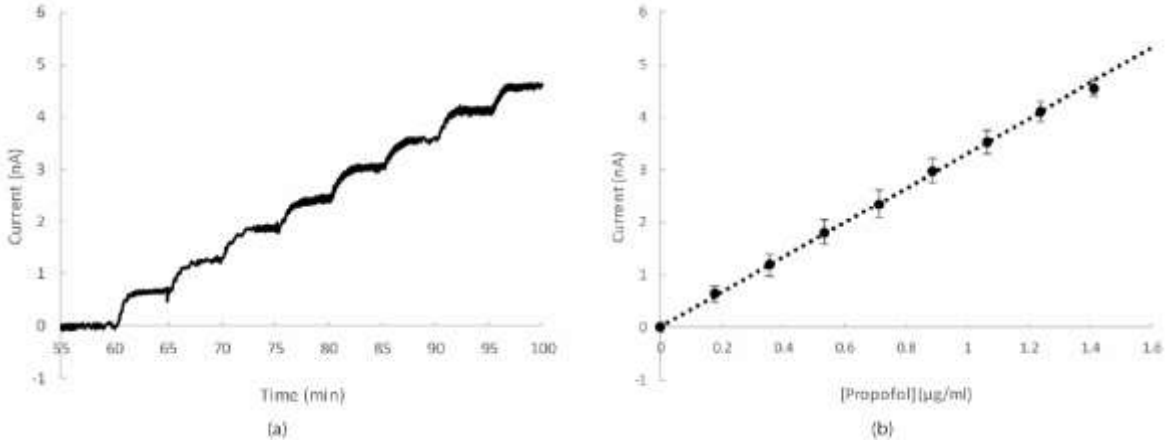

Fig. 3 – (a) Amperometric response of functionalized electrode with successive injections of 20 μl of 1 mM propofol solution. Potential is +0.6 V vs. screen-printed Ag/AgCl. Solution is 10 mM PBS containing 50 μg/ml NADP$^+$ and G6P. (b) Mean of the plateau current (relative to the baseline) against propofol concentration. The error bars represent three standard deviations.

The concentration range shown in Fig. 3 is below the typical therapeutic range for propofol. However, approximately 98% of propofol in human blood is bound to either erythrocytes or serum proteins, with only the remaining 2% existing free in solution [20]. Therefore, the relevant testing range for a potential point-of-care propofol sensor in a real-world setting will likely be far below that of the therapeutic range, and this is a more meaningful range over which to assess the sensor's performance. The response of the sensor has been shown to be stable for up to 10 days from fabrication when stored at 4°C, with sensors tested over this time period showing no apparent decrease in sensitivity (Supplementary data, Fig. S1) and no signs of electrode fouling. The coefficient of variation for the sensitivity of the sensors tested over this time period was 0.09.

The limit of detection of 67 ng/ml compares favorably with that of alternative reported propofol detection techniques. It falls within the range of reported values for techniques such as HPLC [21] [22] and GC/MS [23] [24], and whilst these techniques can achieve greater sensitivity, they are complex, expensive and incapable of continuous measurement. The limit of detection for this technique is also lower than that reported for emerging optical techniques such as spectrophotometry [10] and fluorescence spectrometry [11], neither of which have been demonstrated as being applicable to continuous, real-time measurement. It also compares favorably with other electrical and electrochemical approaches. It is lower than the detection limit achieved using a chemiresistive molecularly imprinted polymer (MIP), as reported by Hong *et al.* [25]. An approach that, to date, has only been demonstrated for discrete rather than continuous measurement. This limit of detection is an order of magnitude lower than achieved by voltammetry with machine learning fouling compensation, as reported by Aiassa *et al.* [14], and while this approach has been demonstrated for continuous monitoring of propofol, it has only been demonstrated up to a period of ten minutes, rather than the hours more typical of procedures requiring general anesthesia. A summary of other reported techniques and how their detection limits compare is shown in Table 1.

Approach	**Limit of detection (ng/ml)**	**Medium**	**Reference(s)**
HPLC	1 – 250	Buffer/blood	[21] [22]
GC/MS	2.5 – 110	Urine/blood	[23] [24]
Spectrophotometry	270	Blood	[10]
Fluorescence spectroscopy	500	Buffer	[11]
Chemiresistive MIP	100	Plasma	[25]
Voltammetry with fouling correction	428	Buffer	[14]
Cytochrome P450 2B6 amperometric biosensor	67 ± 7	Buffer	This study

Table 1 – Summary of reported limits of detection for various propofol detection and quantification techniques. Where limits of quantification were stated in preference to limits of detection, the limit of detection has been assumed to be one third of the limit of quantification.

Other groups have reported enzyme-based electrochemical sensors for the detection of phenolic molecules. One such example is Nazari *et al.* who have demonstrated laccase-based sensors for the detection of catechol in water [26] [27] [28]. This group has investigated several different methods of immobilizing the enzyme and have achieved limits of detection ranging between approximately 3.5 and 228 ng/ml. The limit of detection of the sensor reported here falls within this rage. However, this group have mostly reported discrete, rather than continuous, measurement, so it is unclear how significant an issue electrode fouling will prove for laccase-based sensors.

In order to assess the performance of the sensor in conditions closer to the physiological, the amperometric response of the sensor was obtained in a solution consisting of 50 µg/ml of $NADP^+$ and G6P, and 5 wt% BSA in 10 mM PBS (2.7 mM KCl, 137 mM NaCl, pH 7.4). This solution is considered "serum-like" as it possesses physiological salinity [29], pH [30] and albumin concentration [31]. It can

be seen from Fig. 4 that the sensor produces a linear response across the therapeutic range. The sensitivity (0.64 ± 0.02 nA/µg/ml/mm^2) is reduced and the limit of detection (262 ± 54 ng/ml) is increased when compared to the response in the PBS solution, but as stated previously, this is to be expected as the majority of the propofol will bind to the albumin and thus be prevented from reaching the sensor surface. However, the limit of detection is still comfortably below the lower end of the therapeutic range. There is no discernable change in the response time of the sensor between the buffer solution and the BSA solution (Supplementary data, Fig. S2).

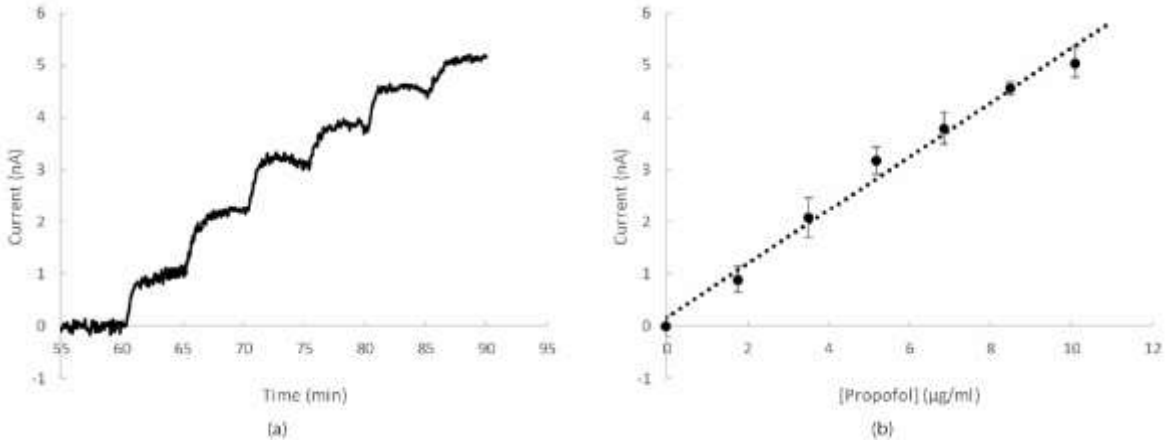

Fig. 4 – (a) Amperometric response of functionalized electrode in serum-like solution with successive injections of 200 µl of 1mM propofol solution. Potential is +0.6 V vs. screen-printed Ag/AgCl. Solution is 10 mM PBS containing 5 wt% BSA, 50 µg/ml $NADP^+$ and G6P. (b) Mean of the plateau current (relative to the baseline) against propofol concentration. The error bars represent three standard deviations.

Amperometric measurements were performed while injecting solutions of ascorbic acid and lidocaine (Fig. 5). It can be seen that increasing concentration of ascorbic acid (i-iii) produces a slight increase in current, but far below that produced by equivalent concentrations of propofol (vii-ix). Injections of lidocaine solution (iv-vi) produced no observable change in current. Ascorbic acid was chosen as it is well documented to be a common source of interference for electrochemical biosensors [32], being easily oxidized and the most common electroactive biological molecule [33]. Lidocaine is significant as, in addition to being commonly used as part of general anesthesia [34] [35], it is another substrate of the enzyme cytochrome P450 2B6 [36]. The typical ranges of both ascorbic acid and lidocaine are of a similar order of magnitude to the therapeutic range of propofol [19]. It is clear from Fig. 5 that the functionalized electrodes demonstrate high specificity toward these two potential sources of interference.

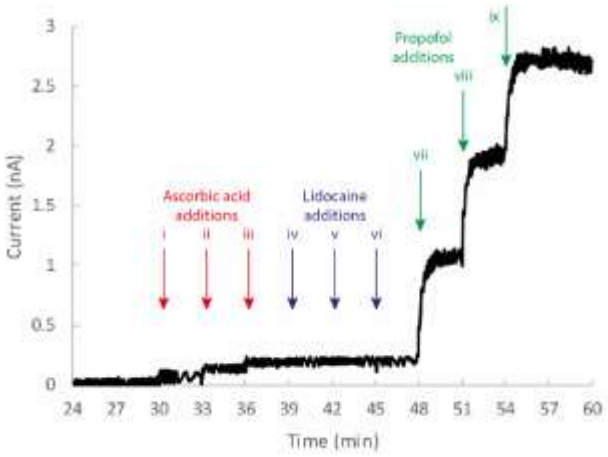

Fig. 5 – Amperometric response of functionalized electrode with successive injections of ascorbic acid solution (i-iii: 0.18, 0.35 and 0.53 µg/ml respectively), lidocaine solution (iv-vi; 0.23, 0.47 and 0.70 µg/ml respectively) and propofol solution (vii-ix; 0.18, 0.35 and 0.53 µg/ml respectively). Potential is +0.6 V vs. screen-printed Ag/AgCl. Solution is 10 mM PBS containing 50 µg/ml $NADP^+$ and G6P.

Fig. 6a shows the results of amperometry measurements in the absence of $NADP^+$ and G6P. These experiments serve as a control for the contribution of the enzyme, as in the absence of these cofactors the enzyme will not catalyze the conversion of propofol as it will no longer have a source of electrons. Therefore, the increases in current observed after the addition of propofol solution are the result of the direct electrochemical oxidation of the propofol. In the first run it can be seen that after the fourth injection of propofol (corresponding to a concentration of approximately 0.7 µg/ml) there is a clear trend of decreasing current with time, suggestive of electrode fouling. This is even more apparent in Fig. 6b, in which it can be seen that the current response plateaus at approximately 1 µg/ml of propofol, a value that is well within the linear range of the sensor as discussed previously. Repeated measurements, performed using the same electrode on successive days, show a similar response but at significantly reduced sensitivities. The third run with the electrode has a sensitivity that is 22% that of the first run. These results are clear evidence of fouling of the electrode by propofol oxidation, fouling that does not occur in the presence of $NADP^+$ and G6P, where propofol is converted by the enzyme. Similar experiments performed with the addition of $NADP^+$ and G6P result in the sensor showing a sensitivity on the third run that is approximately 95% of that on the first run with a coefficient of variation of 0.09 (Supplementary data, Fig. S3). Similar fouling effects are seen for electrodes fabricated in an identical manner, only without the inclusion of the CypExpress 2B6, (Supplementary data, Fig. S4) confirming that these effects are the result of propofol not being converted to the quinone/quinol pair by the enzyme.

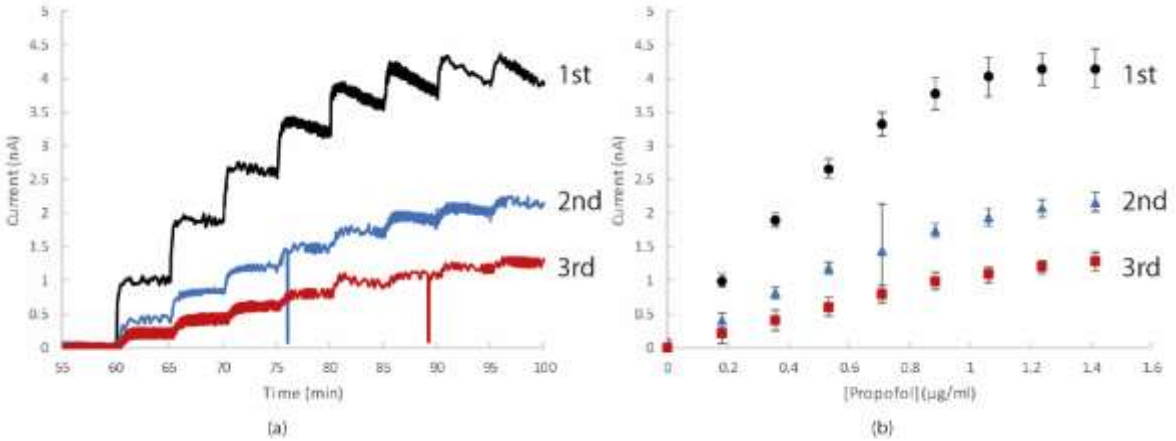

Figure 6 – (a) Amperometric response of electrode with successive injections of 20 µl of 1 mM propofol solution in the absence of NADP+ and G6P for the first, second and third repetitions of the same electrode on successive days. Potential is +0.6 V vs. screen-printed Ag/AgCl, solution is 10 mM PBS. (b) Mean of the plateau current against the propofol concentration. The error bars represent three standard deviations.

It is well documented that gold nanoparticles can help stabilize proteins including enzymes [37] [38] [39]. Sensors fabricated without the addition of the gold nanoparticles display clear signs of electrode fouling at higher propofol concentrations (Fig. 7), indicating that the enzyme has denatured and is no longer converting the propofol as expected. Thus it can be seen that the presence of the gold nanoparticles is essential for maintaining the stability of the cytochrome P450 2B6.

$NADP^+$ and G6P must be present in excess so as to provide a sufficient supply of electrons to the enzyme and not present a limiting factor for the enzymatic conversion of propofol. Amperometric measurements with $NADP^+$ and G6P concentrations of 25 and 10 µg/ml also show signs of electrode fouling at higher propofol concentrations (Supplementary data, Fig. S5).

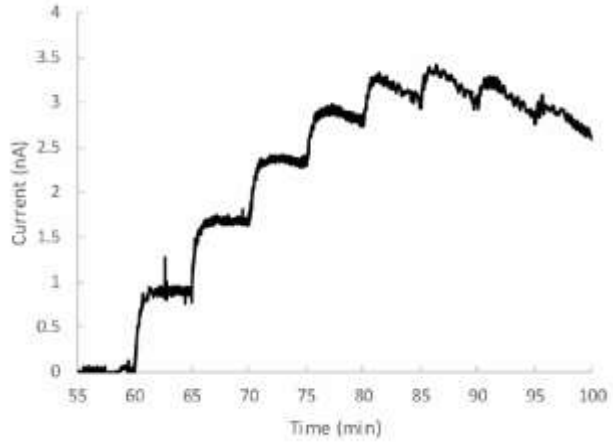

Figure 7 – Amperometric response of electrode functionalized without gold nanoparticles with successive injections of 20 µl of 1 mM propofol solution. Potential is +0.6 V vs. screen-printed Ag/AgCl. Solution is 10 mM PBS containing 50 µg/ml NADP+ and G6P.

4. Concluding remarks

We have demonstrated an enzyme-based propofol biosensor that avoids issues of electrode fouling by converting the propofol into a quinone/quinol redox pair which can be detected via simple electrochemistry. This sensor responds to changes of propofol concentration within one minute, has a limit of detection of 67 ± 7 ng/ml and has been shown to have good specificity towards two potential interfering compounds. The sensor has been demonstrated in a serum-like solution and has a linear response across the therapeutic range of propofol. This sensor represents an important first step in developing an effective means of real-time, point-of-care monitoring of the blood concentration of propofol for general anesthesia patients.

Future work will focus on incorporating the sensor into a suitable analyte recovery system (such as a microdialysis system [40]), allowing for continuous, real-time propofol monitoring without the need for drawing blood, and optimizing the sensor for such an application. There is considerable scope for improving the detection limit of this approach further still, for instance by nanostructuring the electrode surface, switching to micro-scale electrodes or a combination thereof. In addition, the specificity of the sensor in relation to other perioperative drugs will be investigated.

Acknowledgements

The authors would like to thank Dr. Mark O'Connell, Dr. Tim Craft and Prof. John Sear, all of Somnus Scientific Ltd., and Dr. Kevin Honeychurch for their comments and suggestions.

Funding

This work was produced as part of an Innovate UK Biomedical Catalyst Award, No. 133875: Real-Time Blood Propofol Monitoring.

References

[1] F. Kivlehan, E. Chaum, E. Lindner, "Propofol detection and quantification in human blood: the promise of feedback controlled, closed-loop anesthesia," *Analyst*, vol. 140, pp. 98–106, 2015, 10.1039/C4AN01483A.

[2] M. M. Sahinovic, M. M. R. F. Struys, A. R. Absalom, "Clinical pharmacokinetics and pharmacodynamics of propofol," Clin. Pharmacokinet., vol. 57, pp. 1539–1558, Jul., 2018, DOI. 10.1007/s40262-018-0672-3.

[3] T. Laurila, T. Sorvajarvi, J. Saarela, J. Toivonen, D. W. Wheeler, L. Ciaffoni, G. A. D. Ritchie, C. F. Kaminski, "Optical detection of the anesthetic agent propofol in the gas phase," Anal. Chem., vol. 83, no. 10, pp. 3963-3967, May, 2011, DOI. 10.1021/ac200690f.

[4] T. J. Wigmore, K. Mohammed, S. Jhanji, "Long-term survival for patients undergoing volatile versus IV anesthesia for cancer surgery," Anesthesiol., vol. 124, no. 1, pp. 69-79, Jan., 2016, DOI. 10.1097/ALN.0000000000000936.

[5] M. Campbell, M. T. Pierce, "Atmospheric science, anaesthesia and the environment," BJU Edu., vol. 15, no. 4, pp. 173-179, Oct., 2015, DOI. 10.1093/bjaceaccp/mku033.

[6] M. K. Vollmer, T. S. Rhee, M. Rigby, D. Hifstetter, M. Hill, F. Schoenenberger, S. Reimann, "Modern inhalation anesthetics: Potent greenhouse gases in the global atmosphere," Geophys. Res. Lett., vol. 42, no. 5, pp. 1606-1611, Mar., 2015, DOI. 10.1002/2014GL062785.
[7] C. Hornuss, S. Praun, J. Villigner, A. Dornauer, P. Moehnle, M. Dolch, E. Weninger, A. Chouker, C. Feil, J. Briegel, M. Thiel, G. Schelling, "Real-time monitoring of propofol in expired air in humans undergoing total intravenous anesthesia," Anesthesiol., vol. 106, no. 4, pp. 665-674, Jan., 2007, DOI. 10.1097/01.anes.0000264746.01393.e0.
[8] F. Zhang, H. Dong, X. Zhang, J. Guo, Y. Liu, C. Zhou, X. Zhang, J. Liu, M. Yan, X. Chen, "A non-invasive monitoring of propofol concentration in blood by a virtual surface acoustic wave sensor array," Anal. Sci., vol. 33, no. 11, pp. 1271-1277, Nov., 2017, DOI. 10.2116/analsci.33.1271.
[9] F. Vaiano, G. Serpelloni, M. Focardi, A. Fioravanti, F. Mari, E. Bertol, "LC-MS/MS and GC-MS methods in propofol detection: Evaluation of the two analytical procedures," Forensic Sci. Int., vol. 256, pp. 1-6, Nov., 2015, DOI. 10.1016/j.forsciint.2015.07.013.
[10] B. Liu, D. M. Pettigrew, S. Bates, P. G. Laitenberger, G. Troughton, "Performance evaluation of a whole blood propofol analyser," J. Clin. Monit. Comput., vol. 26, pp. 29-36, Jan., 2012, DOI. 10.1007/s10877-011-9330-0.
[11] J. Diao, T. Wang, L. Li, "Graphene quantum dots as nanoprobes for fluorescent detection of propofol in emulsions," Royal Soc. Open Sci., vol. 6, no. 1, p. 181753, Jan., 2019, DOI. 10.1098/rsos.181753.
[12] M. Ferreira, H. Varela, R. M. Torresi, G. Treiliosi-Filho, "Electrode passivation caused by polymerization of different phenolic compounds," Electrochim. Acta, vol. 52, no. 2, pp. 434-442, Oct., 2006, DOI. 10.1016/j.electacta.2006.05.025.
[13] X. Yang, J. Kirsch, A. Simonian, "Modelling analysis of electrode fouling during electrolysis of phenolic compounds," Electrochim. Acta, vol. 94, no. 1, pp. 259-268, Apr., 2013, DOI. 10.1016/j.electacta.2013.01.019.
[14] S. Aiassa, I. N. Hanitra, G. Sandri, T. Totu, F. Grassi, F. Criscuolo, G. De Micheli, S. Carrara, D. Demarchi, "Continuous monitoring of propofol in human serum with fouling compensation by support vector classifier," Biosens. Bioelectron., vol. 171, p. 112666, Jan., 2021, DOI. 10.1016/j.bios.2020.112666.
[15] Y. Oda, N. Hamaoka, T. Hiroi, S. Imaoka, I. Hase, K. Tanaka, Y. Funae, T. Ishizaki, A. Asada, "Involvement of human liver cytochrome P4502B6 in the metabolism of propofol," Br. J. Clin. Pharmacol., vol. 51, no. 3, pp. 281-285, Mar., 2001, DOI. 10.1046/j.1365-2125.2001.00344.x.
[16] N. Shioya, Y. Ishibe, S. Shibata, H. K. S. Makabe, N. Matsumoto, G. Takahashi, Y. Yamada, S. Endo, "Green urine discoloration due to propofol infusion: A case report," Case Rep. Emerg. Med., vol. 2011, p. 242514, Dec., 2001, 10.1155/2011/242514.
[17] J. Dong, P. L. Carpinone, G. Pyrgiotakis, P. Demokritou, B. M. Moudgil, "Synthesis of precision gold nanoparticles using Turkevich method," Kona, vol. 37, pp. 224-232, Jan., 2020, DOI. 10.14356/kona.2020011.
[18] M. Quan, D. Sanchez, M. F. Wasylkiw, D. K. Smith, "Voltammetry of quinones in unbuffered aqueous solution: Reassessing the roles of proton transfer and hydrogen bonding in the aqueous electrochemistry of quinones," J. Am. Chem. Soc., vol. 129, no. 42, pp. 12847-12856, Oct., 2007, DOI. 10.1021/ja0743083.
[19] R. Regenthal, M. Krueger, C. Koeppel, R. Preiss, "Drug levels: Therapeutic and toxic serum/plasma concentrations of common drugs," J. Clin. Monit. Comput., vol. 15, pp. 529-544, Dec., 1999, DOI. 10.1023/a:1009935116877.
[20] J. X. Mazoit, K. Samii, "Binding of propofol to blood components: implications for pharmacokinetics and for pharmacodynamics," Br. J. Clin. Pharmacol., vol. 47, no. 1, pp. 35-42, Jan., 1999, DOI. 10.1046/j.1365-2125.1999.00860.x.
[21] X. Cussonneau, E. De Smet, K. Lantsoght, J.-P. Salvi, "A rapid and simple HPLC method for the analysis of propofol in biological fluids," J. Pharm. Biomed. Anal., vol. 44, no. 3, pp. 680-682, Nov., 2007, DOI. 10.1016/j.jpba.2006.10.020.
[22] K. Vishwananthan, J. T. Stewart, "HPLC determination of a propofol and remifentanil mixture," J. Chromatogr. Relat. Technol., vol. 22, no. 6, pp. 923-931, 1999, DOI. 10.1081/JLC-100101708.
[23] W. Hikiji, K. Kudo, Y. Usumoto, A. Tsuji, N. Ikeda, "A simple and sensitive method for the determination of propofol in human solid tissues by gas chromatography-mass spectrography," J. Anal. Toxicol., vol. 34, no. 7, pp. 389-393, Sep., 2010, DOI. 10.1093/jat/34.7.389.
[24] S. Y. Lee, N.-H. Parl, E.-K. Jeong, J.-W. Wi, C.-J. Kim, J. Y. Kim, M. K. In, J. Hong, "Comparison of GC/MS and LC/MS methods for the analysis of propofol and its metabolites in urine," J. Chromatogr. B, vol. 900, no. 1, pp. 1-10, Jul., 2012, DOI. 10.1016/j.jchromb.2012.05.011.
[25] C-C. Hong, C-C. Lin, C-L. Hong, Z-X. Lin, M-h. Chung, P-W Hsieh, "Handheld analyzer with on-chip molecularly-imprinted biosensors for electrical detection of propofol in plasma samples," Biosens. Bioelectron., vol. 86, pp. 623-629, Dec., 2016, DOI. 10.1016/j.bios.2016.07.032.
[26] M. Nazari, S. Kashanian, R. Rafipour, "Laccase immobilization on the electrode surface to design a biosensor for the detection of phenolic compound such as catechol," Spectrochim Acta Part A, vol. 145, pp. 130-138, Feb., 2015, DOI. 10.1016/j.saa.2015.01.126.
[27] N. Maleki, S. Kashanian, E. Maleki, M. Nazari, "A novel enzyme based biosensor for catechol detection in water samples using artificial neural network," Biochem. Eng. J., vol. 128, pp. 1-11, Dec., 2017, DOI. 10.1016/j.bej.2017.09.005.
[28] M. Nazari, S. Kashanian, N. Maleki, N, Shahabadi, "Laccase immobilized onto graphene oxide nanosheets and electrodeposited gold-cetyltrimethylammonium bromide complex to fabricate a novel catechol biosensor," Bull. Mater. Sci., vol. 42, p. 51, Feb., 2019, DOI. 10.1007/s12034-018-1717-9.
[29] C. Opoku-Okrah, B. K. S. Acquah, E. E. Dogbe, "Changes in potassium and sodium concentrations in stored blood," Pan Afr. Med. J., vol. 20, p. 236, Mar., 2015, DOI. 10.11604/pamj.2015.20.236.5851.

[30] O. Brørs, S. Jacobsen, “pH lability in serum during equilibrium dialysis,” Br. J. Clin. Pharmac., vol. 20, no. 1, pp. 85-88, Jul., 1985, DOI. 10.1111/j.1365-2125.1985.tb02803.x.
[31] J. W. Kim, M. S. Byun, J. H. Lee, D. Yi, S. Y. Jeon, B. K. Sohn, J-Y. Lee, S. A. Shin, Y. K. Kim, K. M. Kang, C-H. Sohn, D. Y. Lee, “Serum albumin and beta-amyloid deposition in the human brain,” Neurology, vol. 95, no. 7, pp. e815-e826, Aug., 2020, DOI. 10.1212/WNL.0000000000010005.
[32] Q. H. Meng, W. C. Irwin, J. Fesser, K. L. Massey, “Interference of ascorbic acid with chemical analytes,” Ann. Clin. Biochem., vol. 42, no. 6, pp. 475-477, Nov., 2005, DOI. 10.1258/000456305774538274.
[33] A. M. Pisoschi, A. Pop, A. I. Serban, C. Fafaneata, “Electrochemical methods for ascorbic acid determination,” Electrochim. Acta, vol. 121, pp. 443-460, Mar., 2014, DOI. 10.1016/j.electacta.2013.12.127.
[34] J.-H. Bahk, Y.-J. Lim, “Using intracuff lidocaine during general anesthesia,” Anesth. Analg., vol. 92, no. 4, pp. 1073-1077, Apr., 2001, DOI. 10.1097/00000539-200104000-00058.
[35] F. R. Altermatt, D. A. Bugedo, A. E. Delfino, S. Solari, I. Guerra, H. R. Munoz, L. I. Cortinez, “Evaluation of the effect of intravenous lidocaine on propofol requirements during total intravenous anaesthesia as measured by bispectral index,” Br. J. Anaesth., vol. 108, no. 6, pp. 979-983, Jun., 2012, DOI. 10.1093/bja/aes097.
[36] S. Imaoka, T. Yamada, T. Hiroi, K. Hayashi, T. Sakaki, Y. Yabusaki, Y. Funae, “Multiple forms of human P450 expressed in saccharomyces cerevisiae,” Biochem. Pharmacol., vol. 51, no. 8, pp. 1041-1050, Apr., 1996, DOI. 10.1016/0006-2952(96)00052-4.
[37] S. Thobhani, S. Attree, R. Boyd, N. Kumarswami, J. Noble, M. Szymanski, R. A. Porter, “Bioconjugation and characterization of gold colloid-labelled proteins,” J. Immunol. Meth., vol. 356, no. 1-2, pp. 60-69, Apr., 2010, DOI. 10.1016/j.jim.2010.02.007.
[38] S. Zhao, X. Ji, P. Lin, Y-M. Liu, “A gold nanoparticle-mediated enzyme bioreactor for inhibitor screening by capillary electrophoresis,” Anal. Biochem., vol. 411, no. 1, pp. 88-93, Apr., 2011, DOI. 10.1016/j.ab.2010.12.025.
[39] F. Gherardi, L. Turyanska, E. Ferrari, N. Weston, M. W. Fay, B. J. Colston, “Immobilized enzymes on gold nanoparticles: From enhanced stability to cleaning of heritage textiles,” ACS Appl. Bio Mater., vol. 2, no. 11, pp. 5136-5143, Oct., 2019, DOI. 10.1021/acsabm.9b00802.
[40] F. Baldini, “Microdialysis-based sensing in clinical applications,” Anal. Bioanal. Chem., vol. 397, pp. 909-916, Mar., 2010, DOI. 10.1007/s00216-010-3626-7.